# Morphology and Mechanical Performance of Polystyrene/Polyethylene Composites Prepared in Supercritical Carbon Dioxide

**Edward Kung, Alan J. Lesser,* and Thomas J. McCarthy***

*Department of Polymer Science and Engineering, University of Massachusetts, Amherst, Massachusetts 01003*

*Received February 2, 1998; Revised Manuscript Received April 24, 1998*

ABSTRACT: Polystyrene/polyethylene composites have been prepared by the heterogeneous radical polymerization of styrene within supercritical carbon dioxide−swollen high density polyethylene (HDPE) substrates. Composition of the composites can be controlled with reaction time and initial ratio of styrene to HDPE. The polystyrene produced within the substrate is of high molecular weight. Differential scanning calorimetry and wide-angle X-ray diffraction indicate that the crystalline portion of the HDPE substrate is unaffected by the procedure used in this investigation. Scanning electron microscopy indicates that the polystyrene resides in the noncrystalline domains and permeates throughout the spherulitic structure of the HDPE substrates. This morphology is very different from the morphology of polystyrene/polyethylene blends produced by conventional melt/mixing techniques. The strengthening of the spherulitic structure of HDPE produces an efficient enhancement in the modulus of the overall composite. The tensile strengths of the composites are dramatically enhanced over conventionally produced blends. The addition of brittle polystyrene to extremely tough HDPE substrates decreases the overall fracture toughnesses of the composites.

## Introduction

Recently there has been a great deal of interest in using supercritical carbon dioxide (SC $CO_2$) as a solvent and/or swelling agent to aid in polymer processing and polymer chemistry.[1−11] $CO_2$ is nonflammable, nontoxic, and relatively inexpensive; the moderate critical conditions for $CO_2$ ($T_c$ = 31.1 °C, $P_c$ = 72.8 atm) make it a convenient fluid for experimentation. While it is known that SC $CO_2$ is a very weak solvent for most polymers—with the exception of some fluoropolymers and silicones—even at extremely high pressures and temperatures,[12] it is a good swelling agent for most polymers and will dissolve many small molecules.[13−16] The density of a supercritical fluid (SCF), and thus its solvent strength, is continuously tunable as a function of temperature or pressure up to liquidlike values. This provides the ability to control the degree of swelling in a polymer[13−15,17,18] as well as the partitioning of small molecule penetrants between a swollen polymer phase and the fluid phase.[19,20] The low viscosity and zero surface tension of a SCF allow for fast mass transfer of penetrants into a swollen polymer. The lack of vapor/liquid coexistence in a SCF allows the sorption to proceed without the penetrant solution wetting the substrate surface. Since most of the common SCFs are gases at ambient conditions, the removal and recovery (if necessary) of the solvent from the final product are extremely facile. All these factors can aid in the production of polymer composites.

A SC solution of a monomer, initiator, and $CO_2$ can be absorbed into a solid polymer substrate, and subsequent polymerization of the monomer yields a composite system of the two polymers. Previous work in our group demonstrated that the infusion and ensuing radical polymerization of styrene within various solid semicrystalline and amorphous polymer substrates were possible.[4,7] The method involved the soaking of the substrate polymer in a SC solution of styrene, a thermal radical initiator, and $CO_2$ at a temperature where the initiator decomposes very slowly. The system is either vented (removing the SC solution) and then heated to initiate polymerization or heated and then vented after polymerization.

The system we examine here is polystyrene/high density polyethylene (HDPE) fabricated using the technique described above. We studied the phase and reaction behavior of this system and examined the morphology of the resulting composites knowing that polystyrene and polyethylene are not miscible polymers and should thus phase separate in some fashion. If the process temperatures remain below the depressed melting temperature of the HDPE substrate, the polymerization of styrene should be confined to the amorphous phase of the substrate and any large scale phase segregation should be frustrated by the crystalline phase. Consequently, we expect interesting mechanical performance from composites with such kinetically trapped morphologies. Herein, we report the results of a detailed study of the syntheses of and resulting composite moduli, strengths, and fracture toughnesses of these systems. We also examined how the addition of polystyrene to HDPE alters the micromechanics of failure in precracked specimens.

## Experimental Section

**Materials.** Substrate samples were prepared by compression molding commercially available HDPE (Dow 04452N) pellets into nominally 1.25 mm thick plaques at 250 °C for 4 min and annealing these plaques at 110 °C for 24 h. These plaques were subsequently cut into appropriate sized specimens. Styrene (Aldrich) was vacuum distilled from calcium hydride. Ethylbenzene and *tert*-butyl perbenzoate (TBPB) were used as received from Aldrich. Coleman-grade (99.99% pure) $CO_2$ was either used as received from Merriam-Graves or purified by flowing through columns packed with activated alumina and a copper catalyst (Engelhard Q-5) to remove water and oxygen, respectively.

**Phase Behavior.** We determined the phase behavior of the HDPE/styrene/$CO_2$ system in the same manner described

S0024-9297(98)00140-5 CCC: $15.00 
Published on Web 06/09/1998

in our previous publications[4,7] and that of Berens et al.[15] Modeling mass uptake data as Fickian diffusion into a planar sheet provided the sorption diffusivity of the monomer.[21] Ethylbenzene (a nonpolymerizing styrene analog) was used as the penetrant.

**Blend Synthesis.** HDPE specimens were sealed in stainless steel high-pressure vessels together with aliquots of TBPB/styrene solution (0.3 mol % TBPB). The vessels were then purged with $CO_2$ gas, tared, and equilibrated to the soak temperature of 80 °C in a heated bath. A heated high-pressure $CO_2$ manifold (described elsewhere)[4] was used to pressurize each vessel to 240 atm. This desired pressure was reached in stages; between each stage, the contents were stirred with a vortex mixer and the vessels were reequilibrated to 80 °C. After the final pressurization stage, the vessels were weighed to determine the masses of $CO_2$ transferred and then were allowed to soak for 5 h at 80 °C (conditions that were demonstrated to yield uniform equilibrium infusion). In all cases the styrene in $CO_2$ concentration was 28 wt %. After this initial soaking period, the vessels were equilibrated at the reaction temperature (100 °C) and maintained at this temperature for the desired reaction times. After the prescribed reaction time, the vessels were vented, refilled with nitrogen gas, and maintained at 100 °C for a 6 h postreaction period.

**Characterization.** The compositions of the composites were determined gravimetrically. Melting endotherms and glass-transition temperatures were determined using a TA Instruments 2910 modulated differential scanning calorimeter (DSC) operated with a 3 °C/min ramp rate, a 0.75 °C oscillation amplitude, and a 60 s oscillation period. Wide-angle X-ray diffraction (WAXD) was performed on a Siemens D500 diffractometer.

Phase morphology was determined by two methods. Both methods required that the specimens first be cryomicrotomed at −120 °C to produce flat and relatively featureless surfaces. In method I, the specimens were stained by exposure to ruthenium tetraoxide vapor for 5 min. The ruthenium tetraoxide was purchased as a 0.5% aqueous solution from Electron Microscopy Sciences. The specimens were carbon coated (approximately 100 Å) and examined under a JEOL 6320F field emission scanning electron microscope (SEM) in the backscattered electron imaging (BEI) mode. In method II, the microtomed surfaces were etched in a solution of potassium permanganate, sulfuric acid, and orthophosphoric acid.[22] The etched samples were gold coated (approximately 200 Å) and examined under a JEOL 35CF SEM in the normal secondary electron imaging (SEI) mode.

Determination of the molecular weights of the polystyrene synthesized involved separating the polystyrene and polyethylene. First, the blend specimens were completely dissolved in hot xylenes at 120 °C. This solution was precipitated into a 2:1 (v:v) mixture of acetone and cyclohexane. The precipitate (presumably polyethylene) was removed by filtration, and the remaining solution was rotary evaporated to isolate the polystyrene. The polystyrene was analyzed using a Polymer Laboratories gel permeation chromatograph (GPC), with THF as the mobile phase, to determine molecular weights. The molecular weight of the substrate HDPE was determined using high temperature (145 °C) GPC with 1,2,4-trichlorobenzene as the mobile phase (performed by Lark Enterprises).

All mechanical tests were performed at room temperature on an Instron 1123 mechanical test machine operated at a crosshead speed of 2 mm/min. To determine moduli, rectangular bar specimens were pulled in tension using an extensometer to obtain accurate strain measurements. The initial slopes of the stress−strain curves represent the moduli. For strength measurements, ASTM type V tensile bars (cut after the composites were produced) were pulled in tension, and the maximum tensile stresses attained were taken as the strength values. Single edge notched specimens were used for fracture toughness determination. They were prepared by cutting a notch into a straight rectangular bar, immersing the bar in liquid nitrogen, and then tapping a razor blade into the notch to form a sharp precrack. The specimens ranged in width from 11.8 to 13.2 mm and in thickness from 1.21 to 1.43 mm. The precracks were all nominally 4 mm long.

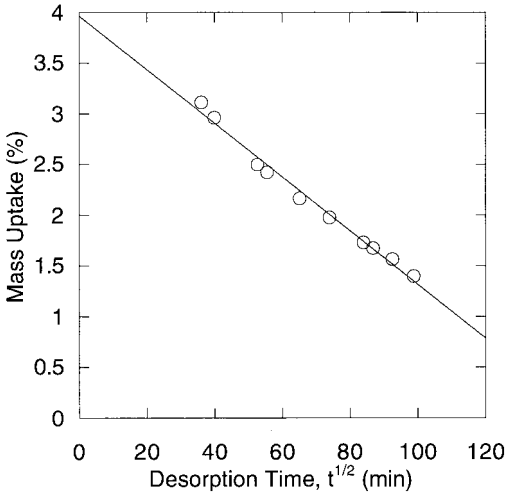


**Figure 1.** A typical ethylbenzene desorption experiment used to determine the equilibrium mass uptake of ethylbenzene in HDPE. The specimen was soaked in a 36 wt % ethylbenzene/$CO_2$ solution for 5 h at 80 °C and 240 atm.

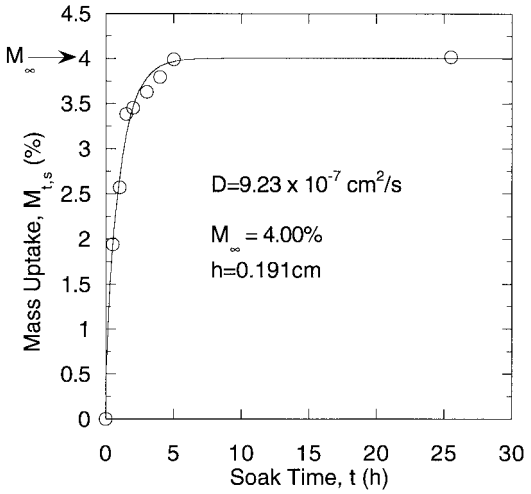


**Figure 2.** Absorption kinetics of ethylbenzene into HDPE for specimens soaked in a 36 wt % ethylbenzene/$CO_2$ solution at 80 °C and 240 atm.

## Results and Discussion

**Phase Behavior and Absorption Kinetics**. On the basis of the work of Suppes and McHugh,[23] all experiments in this study were carried out under conditions where $CO_2$ and styrene exist as a single phase. The solubilities of $CO_2$ and ethylbenzene in HDPE were determined at 80 °C and 240 atm. Ethylbenzene was used as a nonpolymerizing model for styrene. HDPE samples were immersed in either pure $CO_2$ or a 36 wt % ethylbenzene/$CO_2$ solution within pressure vessels under these conditions for various extents of time. Figure 1 shows the results of a typical desorption experiment to determine the mass uptake of ethylbenzene for a given soak period. For ethylbenzene, the equilibrium mass uptake was found to be approximately 4% and was reached after approximately 5 h of soaking; this result was used to set the soak period for the syntheses at 5 h. Figure 2 illustrates the mass uptakes as a function of soak time; the diffusivity of ethylbenzene in $CO_2$-swollen HDPE at the stated conditions was calculated by curve fitting to be 9.23 ×

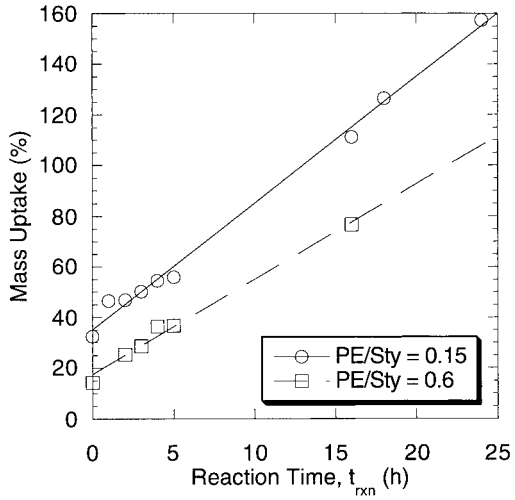


**Figure 3.** Mass uptake of polystyrene into HDPE as a function of reaction time at 100 °C for two concentrations of HDPE. The specimens were soaked in 28 wt % styrene/$CO_2$ for 5 h at 80 °C and 240 atm prior to the reaction period. The specimens were then postreacted under a nitrogen ambient for 6 h at 100 °C after the reaction period.

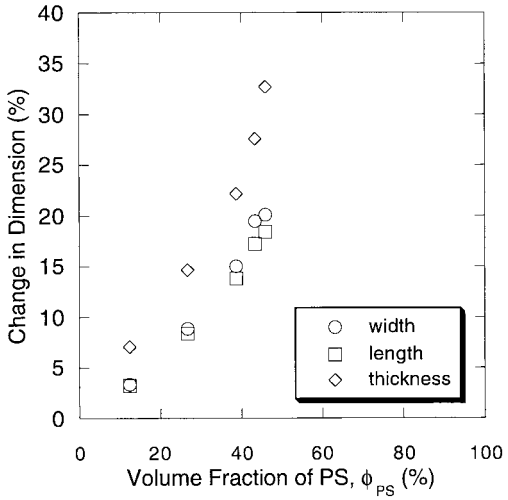


**Figure 4.** Dimensional growth of the specimens over their initial values as a function of polystyrene content.

$10^{-7}$ $cm^2/s$. We also attempted to determine the equilibrium mass uptake of neat ethylbenzene in HDPE at 80 °C, but this experiment was compromised by the fact that neat ethylbenzene slowly dissolves polyethylene under these conditions. Neither $CO_2$ nor ethylbenzene/$CO_2$ was found to dissolve HDPE (or polystyrene) at these conditions.

**Blend Synthesis.** After the HDPE samples were soaked in the styrene/TBPB/$CO_2$ solution for 5 h at 80 °C and 240 atm, the reaction vessels were placed in a 100 °C constant-temperature bath for various durations, vented, and then refilled with nitrogen and maintained at 100 °C for a 6 h postreaction period. Styrene monomer is present in the vessels before the final 6 h postreaction period. The initiator is present in significant concentration throughout this procedure; the reported half-life of TBPB at 100 °C in benzene is approximately 18 h.[24] All experiments were completed within two half-lives of the initiator. In Figure 3, the polystyrene incorporation (as weight percent of substrate) is plotted as a function of reaction time. Data for two sets of experiments are reported; the size and mass of the HDPE samples (and hence the HDPE:styrene ratio) were different in the two sets of experiments. The experiments run with the lower HDPE concentration yielded higher mass uptakes for a given reaction period. The linearity of the data indicates that the reactions are operating in a regime where neither monomer nor initiator depletion of the fluid phase affect composition control; however, this linearity may likely be fortuitous as will be discussed below. The nonzero intercepts at zero reaction time indicate that polymerization occurs during the 5 h soaking period. Clearly, these reaction conditions permit very high polystyrene incorporation and can produce blends with more polystyrene than HDPE. While this raises the interesting question as to the behavior of a system where the substrate becomes the minority component, we have currently limited our study to systems with uptakes below 100%.

We note that the mass uptake data reported in Figure 3 are significantly higher than the equilibrium uptake of styrene expected as a result of the ethylbenzene sorption experiments. The polymerization of styrene within the HDPE substrate is a heterogeneous process; polystyrene is neither soluble in SC $CO_2$ nor miscible with HDPE. As polystyrene forms, it precipitates from the $CO_2$-swollen amorphous HDPE phase and depletes the matrix of styrene. Styrene in the fluid phase repartitions to make up for this depletion; however, this partitioning must also adjust to the creation of a new solid polystyrene phase. This process is continuous as polymerization occurs within the substrate, and partitioning of styrene into the nascent polystyrene phase certainly changes the overall partitioning of styrene between the various solid phases and the fluid phase. These effects allow for the high mass uptakes of polystyrene—well in excess of the equilibrium styrene uptake. The linearity of the data is most likely a function of several properties including the phase behavior and both polymerization and absorption kinetics. Because of the complexity of the system, how these various properties change over time cannot easily be deconvoluted.

We also note that polymerization also occurs outside the substrate. This external polymerization also depletes the fluid phase of styrene and further complicates the system. Interestingly, the polymerization occurring outside the substrate is not nearly as effective as the polymerization occurring within the substrate. This can be discerned in the difference between the molecular weights of the polystyrene formed by the two polymerizations. Molecular weight data are presented below.

**Blend Characterization.** After incorporation of polystyrene, the dimensions of the specimens were found to have grown significantly from their initial substrate dimensions while retaining their original rectangular shape. Plotted in Figure 4 are the extents of dimensional growth as a function of polystyrene content. The higher the polystyrene incorporation, the larger the final dimensions. We have not specifically assessed whether these dimensional increases impart any residual stresses in the final composites. Since SC $CO_2$ acts as a plasticizer, it should have an annealing effect on the specimens and most likely continuously stress relieves the specimens as the dimensional increases occur. We observed no obvious signs of residual stresses during the handling, cutting, or microtoming of the specimens.

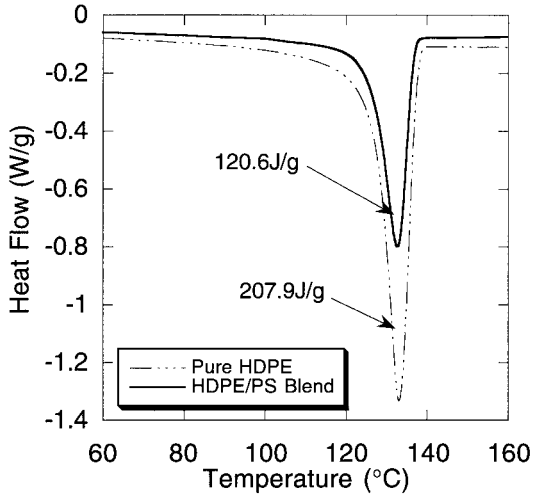


**Figure 5.** Modulated DSC traces showing the melting endotherms for a pure HDPE sample and a 43 wt % polystyrene/HDPE sample. Integration of the endotherms provides the heat of fusion of the samples.

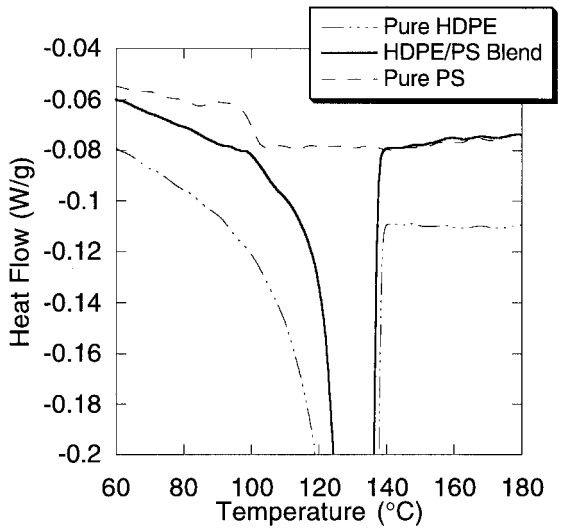


**Figure 6.** Modulated DSC traces showing the glass transition at 100 °C of a pure polystyrene sample and of the polystyrene component of a 43 wt % polystyrene/HDPE sample. The pure HDPE sample exhibited no glass transition in the temperature range shown.

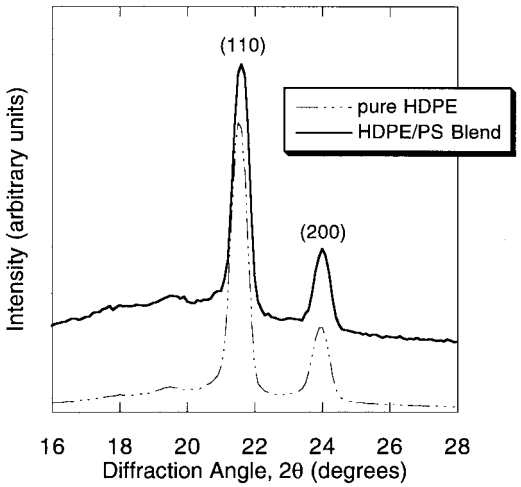


**Figure 7.** WAXD experiments on a pure HDPE specimen and a 39 wt % polystyrene/HDPE specimen. Both the angular positions and breadths of the (110) and (200) peaks of crystalline polyethylene are identical in the two specimens.

Figure 5 shows modulated DSC traces of the virgin HDPE substrate and a 43 wt % polystyrene/HDPE blend. The melting endotherms reveal that the blend synthesis does not affect the crystalline regions of the HDPE substrate. The heat of fusion for polyethylene is known to be 292.65 J/g.[24] By DSC, the unmodified HDPE substrates are 71% crystalline and the 43 wt % polystyrene/HDPE samples are 41% crystalline. The reduction in sample crystallinity is due entirely to dilution by the addition of amorphous polystyrene; the total amount of crystalline HDPE remains unchanged. The melting temperature of the HDPE also remains unchanged. These results indicate that the styrene polymerization occurs solely within the amorphous regions of the polymer. As the temperatures used in the processes are below the depressed melting point of HDPE in the SCF, it is unlikely that penetrants ($CO_2$, monomer or initiator) enter the crystalline regions. The polystyrene glass transition at 100 °C was very faint but discernible when the DSC traces were magnified as shown in Figure 6; a pure polystyrene sample is provided for comparison. Modulated DSC was used because initial normal DSC experiments employing a 10 °C/min ramp rate did not resolve the glass transition of the polystyrene component. In subsequent experiments using normal DSC with a ramp rate of 3 °C/min, the glass transition did appear and the data obtained were identical to that shown for modulated DSC. This is likely due to sensitivity issues with the technique. Wide-angle X-ray diffraction, shown in Figure 7, confirms the DSC data. Both the angular positions and breadths of the diffraction peaks for the (110) and (200) planes of the crystalline polyethylene are identical for a virgin HDPE specimen and for a 39 wt % polystyrene/HDPE blend specimen.

Figure 8 shows scanning electron micrographs of blend samples that were examined using method I (described in the Experimental Section). Ruthenium tetraoxide is known to preferentially stain polystyrene over polyethylene and thus provide phase contrast;[25] the heavy ruthenium atoms backscatter more electrons generating a bright contrast in BEI.[26] Because of the microtomed surfaces, SEI gives almost no information in this case. Figure 9 shows samples examined using method II (described in the Experimental Section). The etchant preferentially attacks polyethylene over polystyrene producing a topography where the polystyrene-rich domains are raised above the polyethylene domains. This preferential oxidation has been verified by control experiments in which pure HDPE and pure polystyrene specimens of equal mass were treated with the etchant for equal times and their mass loss was compared. A pure HDPE specimen examined using method II is displayed in Figure 10.

We note the similarity in morphology revealed by the two techniques. The polystyrene-rich domains reside predominantly at the center of HDPE spherulites and radiate outward. The interlamellae amorphous material provides a location for styrene to penetrate and polymerize. We also note that a considerable amount of polystyrene is present in the center of the spherulites. This is due either to amorphous polyethylene that is present in these locations or to voids that develop during crystallization and/or annealing.[27] It is known that annealing of semicrystalline polymers causes morphological changes to occur. The crystalline lamellae

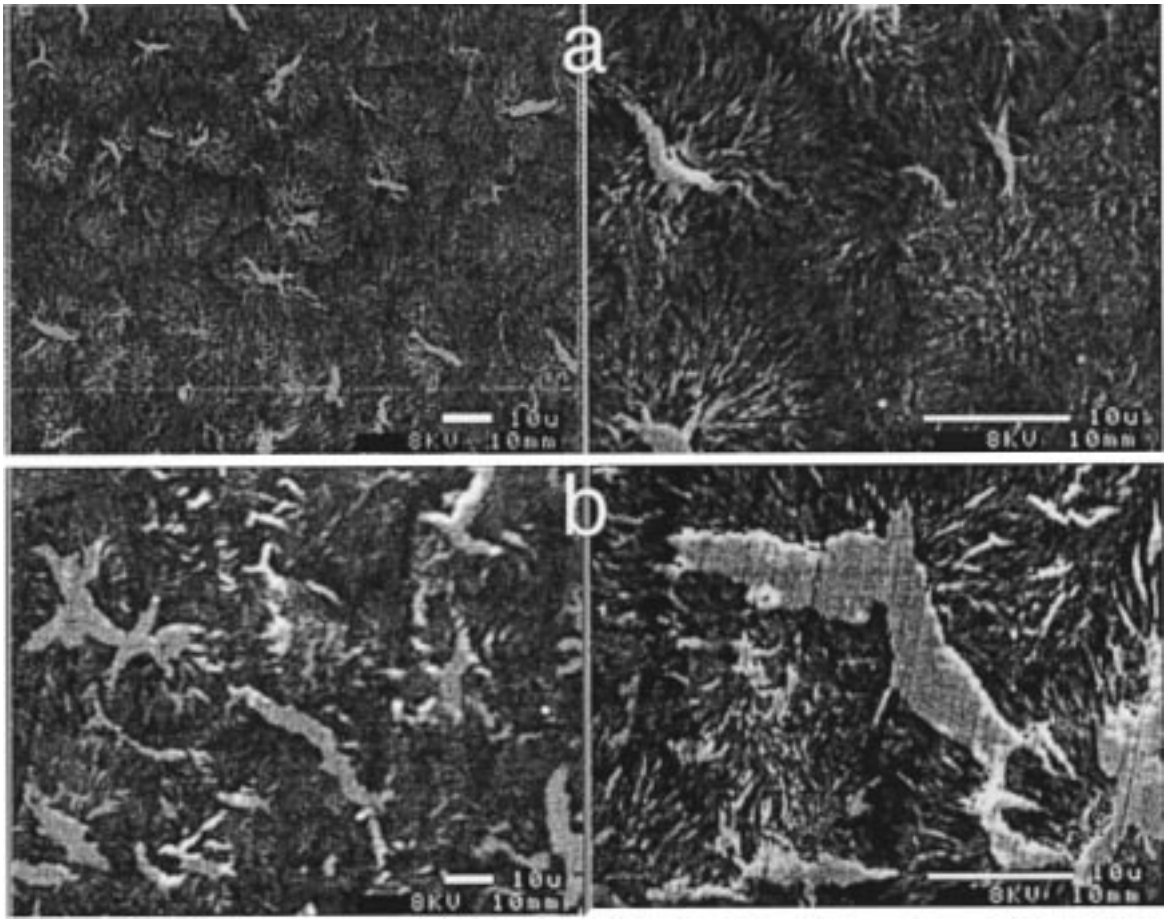


**Figure 8.** Backscattered electron micrographs at two magnifications (note the 10 $\mu$m bars) of polystyrene/HDPE specimens stained with ruthenium tetraoxide vapor: (a) 27 wt % polystyrene; (b) 43 wt % polystyrene. The bright domains are polystyrene rich.

thicken and give rise to an increase in crystallinity and density. The initial spherulite structure, however, may prevent significant volume change from occurring; voiding may occur as a mechanism to offset densification. In single crystals it has been observed that internal voiding occurs during annealing, as material moves from the interior and is incorporated in the larger fold period.[28−30] Whether the spherulite centers contain large amounts of amorphous polymer or voids, this experimental evidence clearly shows that polystyrene is concentrated there.

As polystyrene domains form, the styrene preferentially partitions there, enhancing growth of these domains. The initial polystyrene-rich domains that form "ripen" as is observed in the micrographs. This growth of polystyrene domains appears to break up the spherulites to some degree. A second, finer level, morphology may also exist. The phase separation between the amorphous polystyrene and the amorphous polyethylene is unknown and may be determined by transmission electron microscopy and possibly spin diffusion solid-state NMR experiments.

We also note that the micrographs show no evidence of polystyrene at the spherulite boundaries. This suggests that the polyethylene spherulites in this substrate do not possess distinct boundaries. This lack of discrete boundaries can also be seen in the etched samples of pure polyethylene shown in Figure 10. This morphological characteristic may be affected by the compression molding protocol and the specific grade of polyethylene used. Similar blends prepared with polypropylene substrates show a great deal of polystyrene at the spherulite boundaries, and etched samples of pure polypropylene show sharp, well-defined boundaries between spherulites.[31]

We have not yet eliminated the possibility that some grafting between polystyrene and polyethylene occurs. Substantial amounts of polystyrene (but not all) have been extracted from the "blend" samples by soaking the specimens in refluxing THF for several days. The extracted polystyrene has been characterized as homopolymer by Fourier transform infrared (FTIR) spectroscopy. Nevertheless, this does not eliminate the possibility that grafting occurs to some extent. We suspect that if grafting does occur, it is not a significant contributor to polystyrene mass uptake: all the polystyrene could be extracted from a 50 wt % polystyrene/poly(4-methyl-1-pentene) (PMP) blend that was prepared by essentially the same procedure.[7] The backbone of PMP (with two tertiary C−H bonds per repeat unit) is likely more susceptible to radical grafting than HDPE.

Gel permeation chromatography of polystyrene separated from blend samples indicates that high molecular weight polymer is formed. Polystyrene removed from a 43 wt % polystyrene/HDPE specimen exhibited a $M_w$ = 628K with a PDI ($M_w/M_n$) = 2.7. The corresponding polystyrene formed outside this specimen exhibited a $M_w$ = 48K with a PDI = 3.1. Polystyrene removed from a 27 wt % polystyrene/HDPE specimen exhibited a $M_w$ = 507K with a PDI = 2.9. The corresponding polysty-

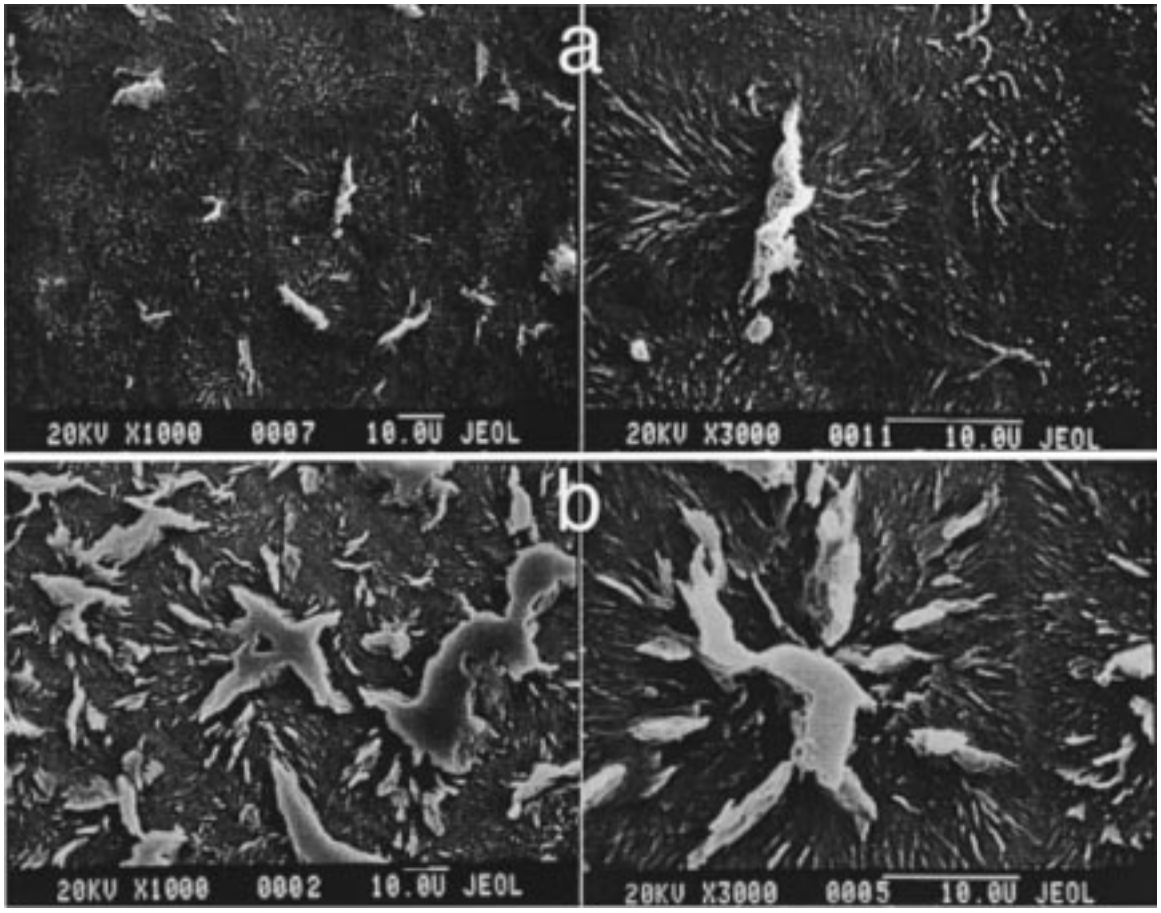


**Figure 9.** Secondary electron micrographs at two magnifications (note the 10 $\mu$m bars) of a polystyrene/HDPE specimen etched in potassium permanganate/acid solution: (a) 27 wt % polystyrene; (b) 43 wt % polystyrene. The raised domains are polystyrene-rich.

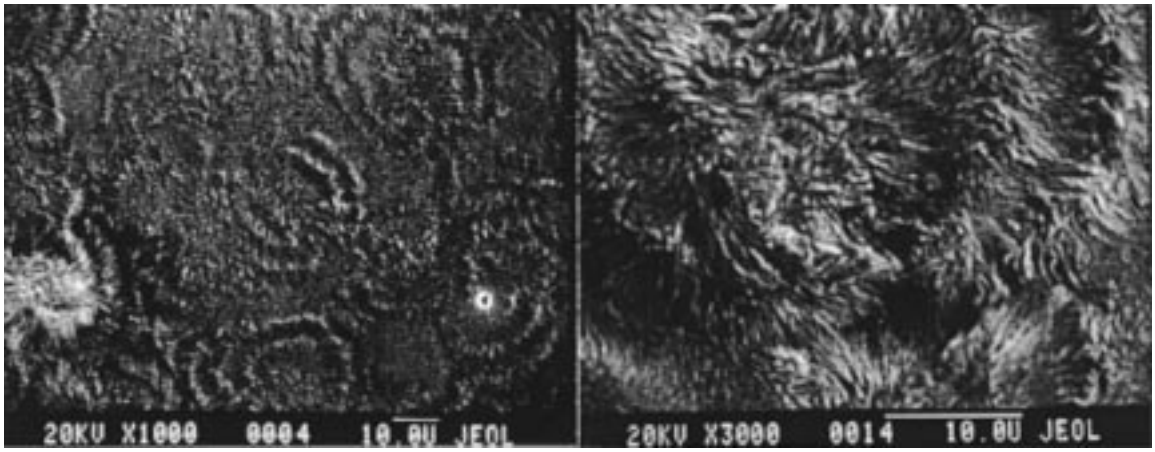


**Figure 10.** Secondary electron micrographs at two magnifications (note the 10 $\mu$m bars) of a pure HDPE specimen etched in potassium permanganate/acid solution showing the initial spherulitic structure of the HDPE substrates.

rene formed outside this specimen exhibited a $M_w = 46K$ with a PDI = 2.0. The HDPE substrate exhibited a $M_w$ = 209K with a PDI = 3.8.

Mechanical tests indicate that these blends do not behave like conventional blends and support our contention that the polystyrene phase is continuous in the substrate. The modulus of the blends as a function of blend composition is plotted in Figure 11. The Voigt and Reuss models (also known as "the rule of mixtures" and "the inverse rule of mixtures," respectively) are provided for comparison.[32] The two models represent the theoretical upper and lower bounds, respectively, on composite modulus behavior; our data follow the Voigt model. The linear Voigt model was derived for a system where the two components of the mixture support load in a parallel fashion. This, in turn, suggests that both the polystyrene and polyethylene phases are continuous. In most conventional melt-blended composites of polystyrene and HDPE, the moduli tend to fall below the Voigt prediction indicating that the phases are discontinuous and dispersed.[33,34]

Figure 12 illustrates the dramatic improvement in tensile strength as polystyrene is incorporated. Note that pure polystyrene fails by brittle fracture rather

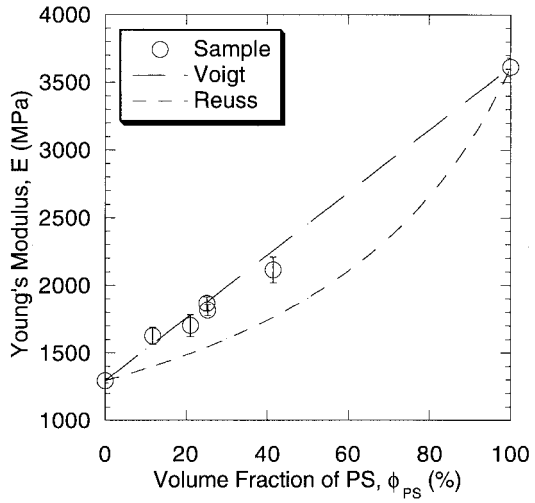


**Figure 11.** Polystyrene/HDPE composite tensile modulus as a function of polystyrene content.

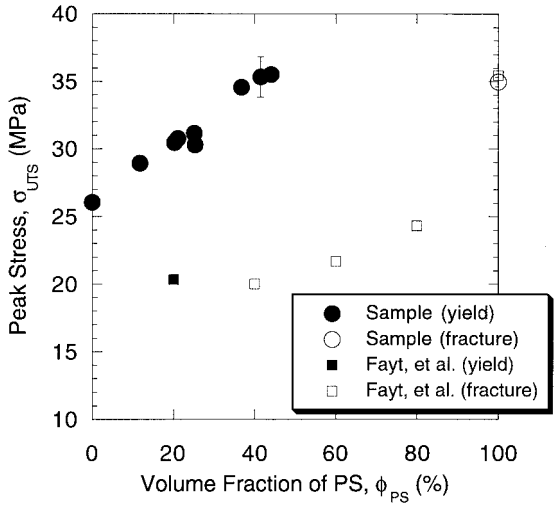


**Figure 12.** Polystyrene/HDPE composite tensile strength as a function of polystyrene content.

than yield in uniaxial tension. Data for conventional melt-blended specimens from Fayt et al.[35] are provided for comparison. Also noteworthy is that the ductile-to-brittle transition for our system is shifted toward a much higher polystyrene content. Fayt and others have shown that polyethylene/polystyrene blends prepared by conventional melt mixing processes without the use of compatibilizers are relatively poor materials.[33,35−37] Blends of certain compositions are even weaker than polystyrene or polyethylene homopolymers. This is due primarily to the poor interfacial adhesion between the two immiscible polymers. Upon deformation, the two phases debond from one another and the dispersed minority phase can no longer support any load. This effectively lowers the load-bearing cross-sectional area. The minority phase domains also act as stress concentrators, further weakening the overall material. From the electron micrographs and the mechanical performance data of the blends that we report here, clearly the polystyrene forms a stiff, reinforcing "scaffold" throughout the spherulites that strengthens the entire structure. The adhesion between the phases is high enough to support load transfer even though the spherulites may appear somewhat broken up. This adhesion may be due to a possible finer morphological structure

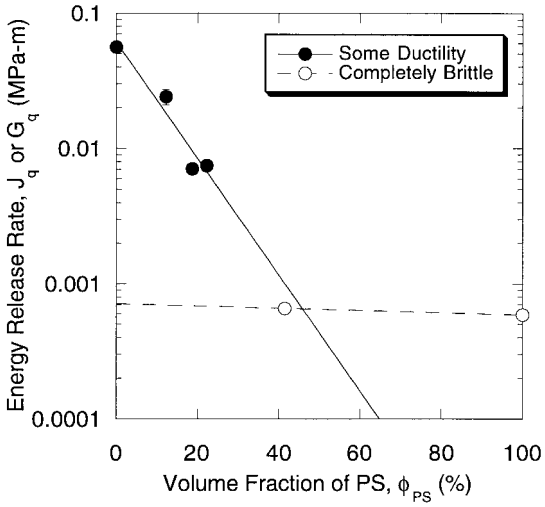


**Figure 13.** Polystyrene/HDPE composite fracture toughness as a function of polystyrene content.

within the polystyrene-rich domains that we have not elucidated.

Linear elastic fracture mechanics (LEFM) was employed to determine the fracture toughnesses for 43 wt % polystyrene and pure polystyrene samples. They behave in a Hookean manner to failure and fail by the unstable growth of the crack upon application of a critical (maximum) stress. The critical stress-intensity factor, $K_q$, was calculated from the initial crack length, $a_0$ (measured under an optical microscope after the fracture test), and the maximum tensile stress, $\sigma_c$, using eq 1, where $b$ is the specimen width.[38]

$$K_q = \sigma_c \sqrt{\pi a_0 \frac{2b}{\pi a} \tan \frac{\pi a_0}{2b}} \frac{0.752 + 2.02\left(\frac{a_0}{b}\right) + 0.37\left(1 - \sin \frac{\pi a_0}{2b}\right)^3}{\cos \frac{\pi a_0}{2b}} \quad (1)$$

The critical energy release rate, $G_q$, can be calculated from the critical stress-intensity factor and the tensile modulus, $E$, of the material using eq 2 (we make the assumption that the specimens were tested in a state of plane stress):

$$G_q = K_q^2/E \quad (2)$$

Elastic plastic fracture mechanics (EPFM) was employed to determine the fracture toughness of all samples that demonstrated ductility during failure. Ductility was defined as a deviation from elastic behavior as evidenced by a curved increase in the stress with strain beyond the elastic limit reaching a peak stress followed by a decrease in the stress. During this nonlinearity in the stress−strain response, the initial crack grew in a stable manner across the ligament of the specimen. Each specimen was strained to a certain crosshead displacement and then unstrained to zero stress. This cycle was repeated several times with progressively larger crosshead displacements. At the end of each cycle, the crack length was measured using an optical microscope. The energy release rate, $J$, for each cycle was calculated from the crack length at the end of each cycle, $a$, and the total area, $U$, under the

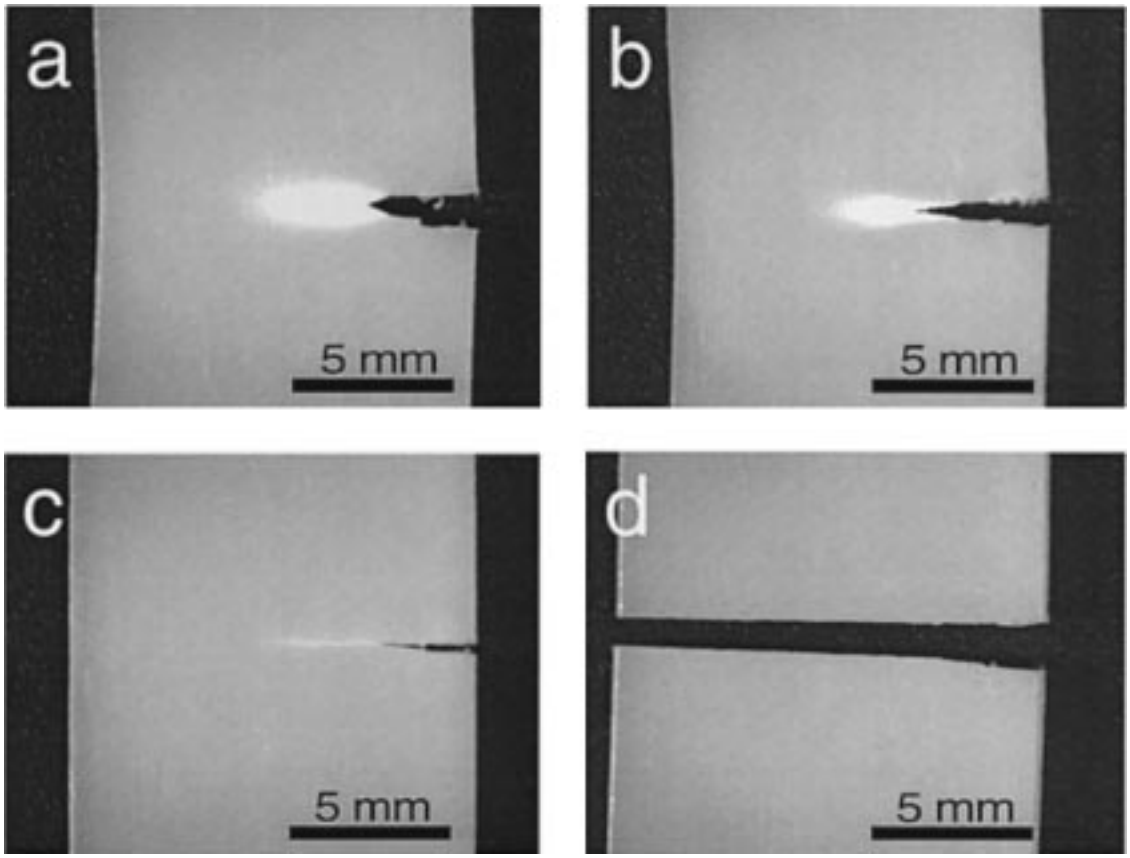


**Figure 14.** Photographs showing the suppression of the damage zone (white) at the crack tips of polystyrene/HDPE blends as the polystyrene content increases: (a) 0 wt % polystyrene; (b) 12 wt % polystyrene; (c) 27 wt % polystyrene; (d) 43 wt % polystyrene.

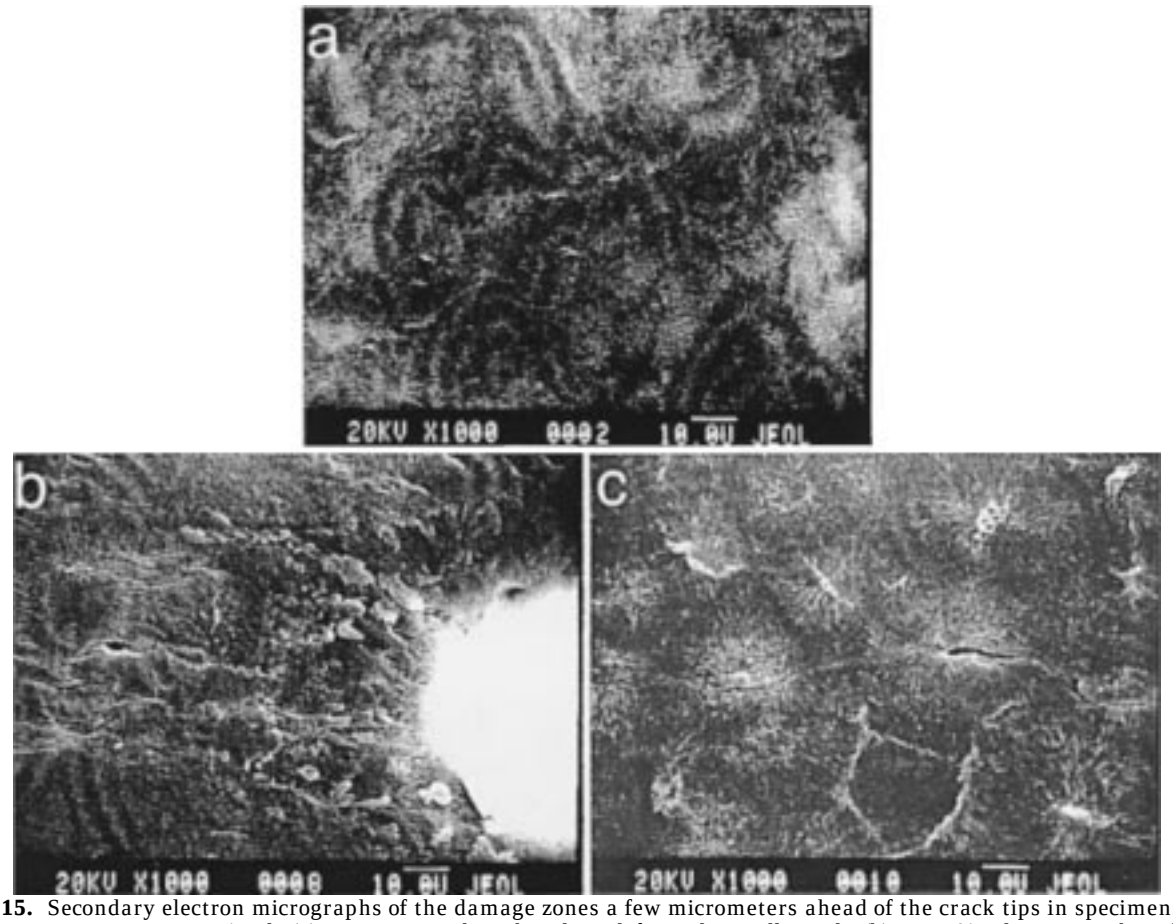


**Figure 15.** Secondary electron micrographs of the damage zones a few micrometers ahead of the crack tips in specimens etched with potassium permanganate/acid: (a) pure HDPE, the spherulites deformed into ellipsoids; (b) 12 wt % polystyrene, the spherulitic structure has been partially destroyed by ductile deformation and some brittle microcracking has occurred; (c) 27 wt % polystyrene, no change in the spherulitic structure occurred, only a single brittle crack traveled through the spherulite centers.

stress−strain curve using eq 3, where $t$ is the specimen thickness.[39]

$$J = \frac{U}{(b-a)t} \frac{1-\frac{a}{b}}{\sqrt{1-2\frac{a}{b}+2\left(\frac{a}{b}\right)^2}} \left[\frac{1-\frac{A}{b}}{\sqrt{1-2\frac{a}{b}+2\left(\frac{a}{b}\right)^2}-\frac{a}{b}}+1\right] \quad (3)$$

The energy release rate was then plotted as a function of crack length extension, and the linear extrapolation of that plot to zero crack extension was taken as the critical energy release rate for the onset of crack growth, $J_q$, for that specimen.

While the material exhibits efficient stiffening and strengthening, there is a loss of fracture toughness. Figure 13 illustrates the dramatic decrease in fracture toughness (critical energy release rate) with the addition of polystyrene. Fracture samples of increasing polystyrene content that were monotonically loaded and then unloaded immediately upon reaching the maximum stress are shown in Figure 14. Macroscopically, one can see how the normally tough polyethylene absorbs a great deal of energy by blunting the crack tip with the formation of a process zone ahead of the crack tip. Incorporation of polystyrene reduces the size of this process zone and thus reduces the ability of the composite to absorb energy during crack growth. In the 27 wt % polystyrene specimens (Figure 14c), the process zone is not macroscopically observable. However, these specimens exhibit stable crack growth under the testing conditions used, and their stress−strain responses show a degree of ductility. The 43 wt % polystyrene (Figure 14d) and pure polystyrene specimens failed similarly: unstable crack growth upon reaching a critical stress.

Electron micrographs of the regions ahead of the crack tips examined using method II are shown in Figure 15. Pure polyethylene spherulites are ductile enough to irreversibly deform into ellipsoids (Figure 15a). In contrast, the 12 wt % polystyrene materials show damage by a more brittle microcracking of the material with some degree of yielding and loss of spherulitic structure (Figure 15b). The 27 wt % polystyrene materials are more brittle; a single crack trajectory travels through the centers of the spherulites without loss or change of the spherulitic structure (Figure 15c). The polystyrene-reinforced spherulites have become strengthened and stiffened to a point that restricts their ability to deform and draw in a ductile fashion. The polystyrene-rich amorphous regions that exist between the crystalline polyethylene lamellae and breakup the center of the spherulites seem to provide accommodating paths for a crack to travel.

## Conclusions

SC $CO_2$ can be employed to aid the infusion of styrene and a radical initiator into HDPE substrates, and interesting composites are prepared by the subsequent polymerization of the styrene within the substrate. By control of the reaction time, the amount of polystyrene that is incorporated into the HDPE substrates can be conveniently controlled to values far in excess of the equilibrium uptake of styrene. This process does not affect the crystalline regions of the HDPE but does affect the spherulitic structure. The styrene must absorb into and polymerize within the amorphous domains of the substrate. The final polystyrene thus possesses a kinetically trapped morphology and can be observed in the amorphous interlamellar regions of the polyethylene spherulites. A great deal of polystyrene also exists in the spherulite centers, implying a certain lack of crystallinity there. The polystyrene thus forms a "scaffold" that reinforces the polyethylene spherulites. This reinforcement is manifested in very efficient modulus enhancement and in dramatic strength improvement as the polystyrene content increases. The penalty for such enhancement is a loss in fracture toughness. The same reinforcement of the spherulitic structure also limits the ductile deformation processes of the structure. This is particularly apparent at the damage zones formed in response to a stress concentration (crack tip). This ductile deformation occurs but is suppressed as polystyrene is added. As more polystyrene is incorporated, the ductile damage mechanism transforms to a more brittle mechanism, and at some point, the brittle polystyrene forms an easy path for a crack to follow.

**Acknowledgment.** We thank the New Materials Synthesis Consortium of the Center for UMass Industry Research on Polymers (AMP, US Army Natick, Loctite, Rexam, Rohm and Haas) and the Office of Naval Research for financial support. Use of the National Science Foundation-sponsored Materials Research Science and Engineering Center central facilities is acknowledged as well.

## References and Notes

(1) DeSimone, J. M.; Guan, Z.; Elsbernd, C. S. *Science* **1992**, *257*, 945.
(2) Adamsky, F. A.; Beckman, E. J. *Macromolecules* **1994**, *27*, 312.
(3) DeSimone, J. M.; Maury, E. E.; Menceloglu, Y. Z.; McClain, J. B.; Romack, T. R.; Combes, J. R. *Science* **1994**, *265*, 356.
(4) Watkins, J. J.; McCarthy, T. J. *Macromolecules* **1994**, *27*, 4845.
(5) Pernecker, T.; Kennedy, J. P. *Polym. Bull.* **1994**, *32*, 537.
(6) Shaffer, K. A.; DeSimone, J. M. *Trends Polym. Sci.* **1995**, *3*, 146.
(7) Watkins, J. J.; McCarthy, T. J. *Macromolecules* **1995**, *28*, 4067.
(8) Romack, T. J.; Maury, E. E.; DeSimone, J. M. *Macromolecules* **1995**, *28*, 912.
(9) Mawson, S.; Johnston, K. P.; Combes, J. R.; DeSimone, J. M. *Macromolecules* **1995**, *28*, 3182.
(10) Mistele, C. D.; Thorp, H. H.; DeSimone, J. M. *J. Macromol. Sci., Pure Appl. Chem.* **1996**, *A33*, 953.
(11) Lepilleur, C.; Beckman, E. J. *Macromolecules* **1997**, *30*, 745.
(12) Rindfleisch, F.; DiNoia, T. P.; McHugh, M. A. *J. Phys. Chem.* **1996**, *100*, 15581.
(13) Wissinger, R. G.; Paulaitis, M. E. *J. Polym. Sci., Part B: Polym. Phys.* **1987**, *25*, 2497.
(14) Berens, A. R.; Huvard, G. S. In *Supercritical Fluid Science and Technology*; Johnston, K. P., Penniger, J. M. L., Eds.; American Chemical Society: Washington, DC, 1989; pp 207−223.
(15) Berens, A. R.; Huvard, G. S.; Korsmeyer, R. W.; Kunig, F. W. *J. Appl. Polym. Sci.* **1992**, *46*, 231.
(16) Shine, A. D. In *Physical Properties of Polymers Handbook*; Mark, J. E., Ed.; American Institute of Physics: Woodbury, NY, 1996; pp 249−256.
(17) Fleming, G. K.; Koros, W. J. *Macromolecules* **1986**, *19*, 2285.
(18) Pope, D. S.; Koros, W. J. *J. Polym. Sci., Part B: Polym. Phys.* **1996**, *34*, 1861.
(19) Shim, J.-J.; Johnston, K. P. *AIChE J.* **1989**, *35*, 1097.
(20) Shim, J.-J.; Johnston, K. P. *AIChE J.* **1991**, *37*, 607.
(21) Crank, J. *The Mathematics of Diffusion*, 2nd ed.; Clarendon Press: Oxford, 1975.
(22) Patrick, M.; Bennett, V.; Hill, M. J. *Polymer* **1996**, *37*, 5335.

(23) Suppes, G. J.; McHugh, M. A. *J. Chem. Eng. Data* **1989**, *34*, 310.
(24) *Polymer Handbook*, 3rd ed.; Brandrup, J., Immergut, E. H., Eds.; John Wiley & Sons: New York, 1989.
(25) Trent, J. S.; Scheinbeim, J. I.; Couchman, P. R. *Macromolecules* **1983**, *16*, 589.
(26) Goizueta, G.; Chiba, T.; Inoue, T. *Polymer* **1992**, *33*, 886.
(27) Matsuoka, S. *J. Appl. Phys.* **1961**, *32*, 2334.
(28) Statton, W. O.; Geil, P. H. *J. Appl. Polym. Sci.* **1960**, *3*, 357.
(29) Geil, P. H. *Polymer Single Crystals*; Wiley-Interscience: New York, 1963.
(30) Holland, V. F. *J. Appl. Phys.* **1964**, *35*, 59.
(31) This work was done in collaboration with Dr. Nathan A. Jones in Professor Alan J. Lesser's research group.
(32) Nielsen, L. E. *Predicting the Properties of Mixtures*; Marcel Dekker: New York, 1978.
(33) Barentsen, W. M.; Heikens, D. *Polymer* **1973**, *14*, 579.
(34) Wycisk, R.; Trochimczuk, W. M.; Matys, J. *Eur. Polym. J.* **1990**, *26*, 535.
(35) Fayt, R.; Jerome, R.; Teyssie, P. *J. Polym. Sci., Part B: Polym. Phys.* **1989**, *27*, 775.
(36) Han, C. D.; Villamizar, C. A.; Kim, Y. W.; Chen, S. J. *J. Appl. Polym. Sci.* **1977**, *21*, 353.
(37) Fayt, R.; Hadjiandreou, P.; Teyssie, P. *J. Polym. Sci.: Polym. Chem. Ed.* **1985**, *23*, 337.
(38) Tada, H.; Paris, P. C.; Irwin, G. R. *The Stress Analysis of Cracks Handbook*, 2nd ed.; Paris Productions, Inc.: St. Louis, MO, 1985.
(39) Williams, J. G. *Fracture Mechanics of Polymers*; John Wiley & Sons: New York, 1984.

MA980140H